The Astrophysical Journal, 688:1118–1123, 2008 December 1


# EMISSION FROM VERY SMALL GRAINS AND PAH MOLECULES IN MONTE CARLO RADIATION TRANSFER CODES: APPLICATION TO THE EDGE-ON DISK OF GOMEZ'S HAMBURGER

Kenneth Wood,[1] Barbara A. Whitney,[2] Thomas Robitaille,[1] and Bruce T. Draine[3]
*Received 2008 March 20; accepted 2008 July 15*

## ABSTRACT

We have modeled optical to far-infrared images, photometry, and spectroscopy of the object known as Gomez's Hamburger. We reproduce the images and spectrum with an edge-on disk of mass 0.3 $M_\odot$ and radius 1600 AU, surrounding an A0 III star at a distance of 280 pc. Our mass estimate is in excellent agreement with recent CO observations. However, our distance determination is more than an order of magnitude smaller than previous analyses, which inaccurately interpreted the optical spectrum. To accurately model the infrared spectrum we have extended our Monte Carlo radiation transfer codes to include emission from polycyclic aromatic hydrocarbon (PAH) molecules and very small grains (VSG). We do this using precomputed PAH/VSG emissivity files for a wide range of values of the mean intensity of the exciting radiation field. When Monte Carlo energy packets are absorbed by PAHs/VSGs, we reprocess them to other wavelengths by sampling from the emissivity files, thus simulating the absorption and reemission process without reproducing lengthy computations of statistical equilibrium, excitation, and de-excitation in the complex many-level molecules. Using emissivity lookup tables in our Monte Carlo codes gives us the flexibility to use the latest grain physics calculations of PAH/VSG emissivity and opacity that are being continually updated in the light of higher resolution infrared spectra. We find our approach gives a good representation of the observed PAH spectrum from the disk of Gomez's Hamburger. Our models also indicate that the PAHs/VSGs in the disk have a larger scale height than larger radiative equilibrium grains, providing evidence for dust coagulation and settling to the midplane.

*Subject headings:* accretion, accretion disks — circumstellar matter — dust, extinction — radiative transfer

## 1. INTRODUCTION

The object known as Gomez's Hamburger (Ruiz et al. 1987) exhibits the spectral and imaging characteristics of an edge-on circumstellar disk. High-resolution *Hubble Space Telescope* (*HST*) imagery shows a bipolar reflection nebula of size $5.5'' \times 2.5''$ bisected by an optically thick dust lane, reminiscent of models and images of disks surrounding low-mass classical T Tauri stars (e.g., Whitney & Hartmann 1992; Burrows et al. 1996; Grosso et al. 2003). The *HST* data support the circumstellar disk (or torus) interpretation first proposed by Ruiz et al. (1987) based on lower resolution optical imaging polarimetry and the object's broadband spectral energy distribution (SED), which is faint in the optical and bright at mid- to far-infrared wavelengths. Such SEDs are characteristic of edge-on circumstellar disks (e.g., Wood et al. 2002). The disk hypothesis for Gomez's Hamburger has been strengthened by recent CO observations (Bujarrabal et al. 2008) that are reproduced with a model of a Keplerian disk of mass 0.9 $M_\odot (d/500\mathrm{pc})^2$, where $d$ is the distance to the source.

Optical spectroscopy of Gomez's Hamburger indicates that the central source is an A0 III star. Using parameters typical to this spectral type and the integrated broadband spectrum, Ruiz et al. (1987) estimated the object to be at a distance of 2.9 kpc with a circumstellar disk of radius 8000 AU. However, as we will show below, the disk is smaller and closer than estimated by Ruiz et al. (1987). This is because they did not take into consideration that the integrated spectrum from an edge-on disk is strongly dependent on inclination (Whitney et al. 2003b). At optical wavelengths edge-on disks are only seen in scattered light and can be several orders of magnitude fainter than systems where the central star is directly seen. In addition to the error in distance determination, the spectral type of the central source may not be accurate because the optical spectrum is entirely scattered light. Therefore, the combination of high-resolution optical spectroscopy and radiation transfer modeling of the scattered starlight from the disk is required for more accurate spectral typing. However, in the absence of higher resolution optical spectroscopy, in our modeling below we adopt the A0 III spectral type from Ruiz et al. (1987).

More recent *Spitzer* Infrared Spectrograph (IRS) observations of Gomez's Hamburger show strong mid-infrared emission features typical of emission from polycyclic aromatic hydrocarbon (PAH) molecules and very small grains (VSGs). Such emission features are common in massive star-forming regions (e.g., Churchwell et al. 2006), as the emission mechanism is sensitive to the strength of the exciting UV radiation from O and B stars. However, charged PAH molecules exhibit significant opacity at optical and infrared wavelengths, so that the PAH excitation may arise from softer photons (Li & Draine 2002), thus enabling PAH emission to be observed from the circumstellar environment of lower mass stars. Indeed, PAH emission has been detected from disks and envelopes around A stars and classical T Tauri stars (e.g., Habart et al. 2004; Pontoppidan et al. 2007; Geers et al. 2006).

In this paper we present models for the *HST* images, broadband SED, and high-resolution *Spitzer* IRS spectrum of Gomez's Hamburger. In doing so, in § 2 we introduce extensions to our Monte Carlo radiation transfer codes that allow us to model emission from PAHs and VSGs. Section 3 presents the radiation transfer modeling of Gomez's Hamburger, and in § 4 we summarize our findings and briefly discuss future applications of our new code developments.

[1] School of Physics and Astronomy, University of St. Andrews, North Haugh, St. Andrews, Fife KY16 9AD, Scotland; kw25@st-andrews.ac.uk.
[2] Space Science Institute, 4750 Walnut Street, Suite 205, Boulder, CO 80301; bwhitney@spacescience.org.
[3] Department of Astrophysical Sciences, Princeton University, Peyton Hall, Princeton, NJ 08544.

## 2. PAH/VSG EMISSION PROCESSES

Emission from PAH molecules and VSGs can dominate the mid-infrared spectrum from dusty regions associated with massive star formation. New mid-infrared images from the *Spitzer Space Telescope* GLIMPSE survey (Churchwell et al. 2004, 2006) dramatically show PAHs acting as a signpost for massive star formation. The characteristic infrared PAH emission spectrum has been studied in detail in many star-forming regions in the Milky Way and other galaxies using a variety of ground- and space-based observatories (e.g., Peeters et al. 2004; Draine et al. 2007). A proper understanding of the infrared emission from star-forming regions and galaxies therefore requires the inclusion of PAHs and VSGs in radiation transfer codes.

Unlike the radiative equilibrium temperatures attained by large dust grains, the absorption and reprocessing of radiation by PAHs and VSGs does not yield an equilibrium temperature. Absorption of a single photon can appreciably increase the energy content of the molecule, and the ensuing radiative de-excitation produces an infrared spectrum consisting of a continuum plus characteristic emission features. Detailed modeling of the emission process therefore requires solving statistical equilibrium in complex multilevel molecules.

Approximations exist for determining the reprocessing of photons and emission from PAHs and VSGs, and have been incorporated into some radiation transfer codes (e.g., Misselt et al. 2001; Pontoppidan et al. 2007; Dullemond et al. 2007a; Manske & Henning 1998). In this paper we introduce a new technique that is readily included into Monte Carlo radiation transfer codes and utilizes the detailed PAH and VSG opacity and emissivity calculations presented by Draine & Li (2007).

### 2.1. *PAH/VSGs in Monte Carlo Radiation Transfer Codes*

Our current Monte Carlo radiation transfer codes (see details in Whitney et al. 2003b) treat multiple anisotropic scattering in three dimensions and calculate radiative equilibrium dust temperatures and spectra using the Bjorkman & Wood (2001) technique or iteratively using methods described by Lucy (1999). The Bjorkman & Wood (2001) technique works well for two- and three-dimensional systems (e.g., Indebetouw et al. 2006), but to determine higher signal-to-noise temperatures for the same number of Monte Carlo energy packets, especially for three-dimensional systems, the techniques described by Lucy (1999) are more efficient (Chakrabarti & Whitney 2007). The Bjorkman & Wood (2001) technique produces the same temperatures and spectra as Lucy's method, but requires more energy packets (or Monte Carlo photons) and hence longer run times for three-dimensional simulations.

Lucy (1999) introduced efficient ways for determining mean intensities and hence temperatures and ionization fractions in Monte Carlo codes by summing the path lengths within grid cells of individual "energy packets" as they take their random walks in the radiation transfer simulation. In particular, the Monte Carlo estimator for the mean intensity in a cell is given by

$$J_i = \frac{\epsilon}{4\pi\Delta t \Delta V_i} \sum l, \tag{1}$$

where $\epsilon = L\Delta t/N$ is the energy of each of the $N$ Monte Carlo energy packets, $L$ is the system luminosity, and $\Delta t$ is the time interval of the Monte Carlo simulation. The summation is over all path lengths, $l$, of energy packets passing through cell $i$ of volume $V_i$. We will make use of this Monte Carlo estimator below.

We have extended our Monte Carlo codes to allow for multiple dust species within any given cell in the simulation grid. When Monte Carlo energy packets interact with dust in a cell, the dust type they interact with is chosen from the relative opacity of each dust species present,

$$P_i = \frac{\rho_i \kappa_i}{\sum_j \rho_j \kappa_j}, \tag{2}$$

where $P_i$ is the probability of the energy packet interacting with dust type $i$, which has density and opacity $\rho_i$ and $\kappa_i$.

If a Monte Carlo energy packet is absorbed by a dust type that attains a radiative equilibrium temperature, the energy packet is reprocessed and the incremental temperature change of the cell is calculated using the Bjorkman & Wood (2001) technique. Therefore at the end of the simulation we have a temperature grid for each dust type that attains radiative equilibrium temperatures.

If however, a Monte Carlo energy packet is absorbed by PAH/VSG opacity, the packet is reprocessed sampling a new frequency from the precomputed emissivity files of Draine & Li (2007). Since the PAH/VSG emissivity has been computed for a wide range of values of the mean intensity of the exciting radiation field, we choose the relevant emissivity file based on the value of the mean intensity in the cell where the Monte Carlo energy packet was absorbed. This requires an iterative procedure whereby on the first iteration energy packets absorbed by PAHs/VSGs are reprocessed using the emissivity file for $J = 1$, where $J$ is the mean intensity relative to the average value for the interstellar radiation field, $J_{\rm ISRF} = 2.17 \times 10^{-2}$ ergs cm$^{-2}$ s$^{-1}$ (Mathis et al. 1983). On subsequent iterations energy packets are reprocessed based on the mean intensity from the previous iteration, calculated using equation (1). Due to the small PAH/VSG fractions in our simulations (typically less than 4%), photons reprocessed by PAHs/VSGs do not contribute significantly to the mean intensity. Therefore we find that this procedure requires at most three iterations for convergence.

### 2.2. *Approximations for PAH/VSG Opacities and Emissivities*

The extensions to our Monte Carlo codes of allowing for multiple dust types mean that in principle we could employ opacity and emissivity files for grains of many different sizes. However, in this first paper we have taken a simpler approach of introducing a cutoff in the grain sizes at $a = 200$ Å, below which we assume grains are transiently heated and energy packets absorbed by these small grains are reprocessed as described above. This is a somewhat arbitrary cutoff, but it is a size above which grains generally attain radiative equilibrium temperatures (Draine & Li 2007).

In addition to introducing a size cutoff between PAH/VSGs and grains in radiative equilibrium, we make the assumption that the PAH/VSG emissivity is a function only of the mean intensity of the radiation field and not the spectral shape of the exciting radiation field. The Draine & Li (2007) emissivities that we use were computed for an exciting radiation field with spectral shape of the model interstellar radiation field of our Galaxy (Mathis et al. 1983). We make this approximation in the absence of emissivity calculations for a wide range of exciting spectra. This is an appropriate first approximation, since the Monte Carlo code accurately treats the transfer and absorption of photons at all wavelengths by the PAH/VSG opacity. So in our technique the correct number of photons are reprocessed by PAHs/VSGs, and their wavelengths are chosen from the precomputed mean intensity-dependent emissivities.

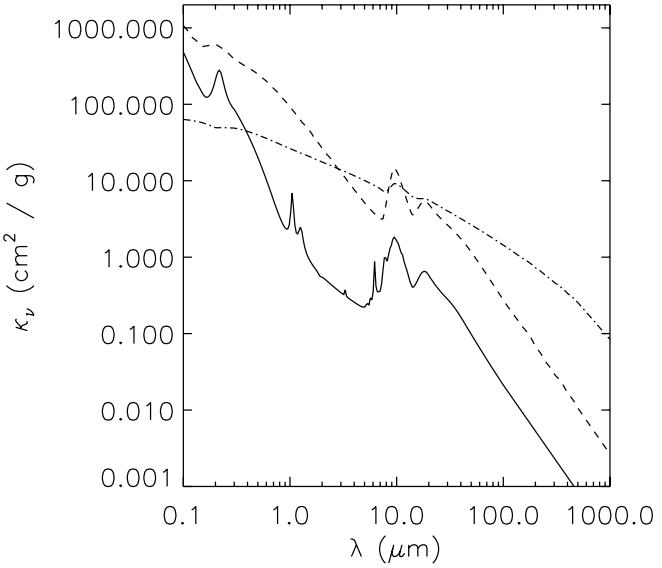


FIG. 1.—*Solid line*: Wavelength-dependent opacity for the PAH/VSG (dust plus gas) model of Draine & Li (2007) for grains with sizes $a < 200$ Å. *Dot-dashed line*: Radiative equilibrium dust model of Wood et al. (2002). For comparison, the dashed line shows the opacity for an ISM dust plus gas mixture.

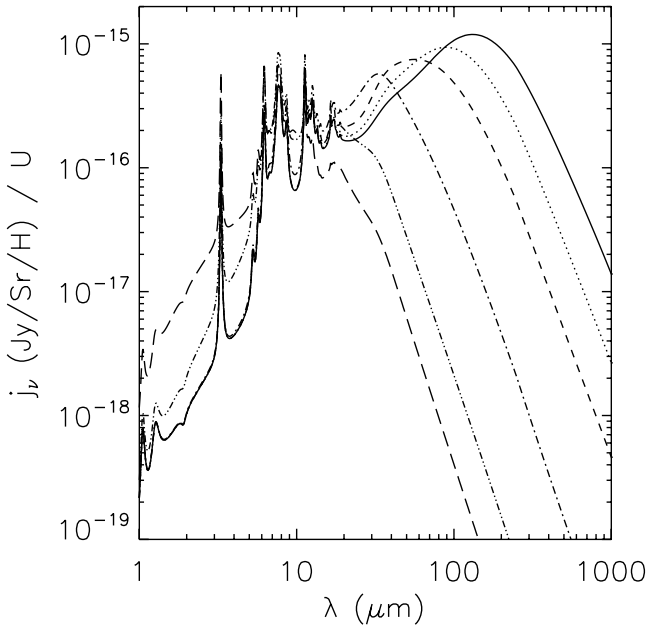


FIG. 2.—Emissivity for PAHs/VSGs with size $a < 200$ Å for different values of $U$, the energy density of the exciting radiation field relative to the average interstellar value. The emissivities shown are in the range $1 \leq U \leq 10^7$. The solid line shows the emissivity for $U = 1$, and the long-dashed line is for $U = 10^7$.

We use the opacity and emissivity files for PAHs/VSGs with sizes $a < 200$ Å taken from the Draine & Li (2007) silicate-graphite-PAH grain model. Their model assumes a power-law grain size distribution with the silicate and graphite abundances, PAH charging, and PAH mass fraction adjusted to reproduce the opacity and infrared spectrum of the Milky Way's diffuse interstellar medium (ISM). In particular they find that a PAH mass fraction of 4.5% is required to reproduce the observed infrared spectra in the Milky Way and other galaxies.

Figures 1 and 2 show the wavelength-dependent opacity and emissivities for PAHs/VSGs with grain sizes $a < 200$ Å. This is the grain size below which we use the described approximation for computing the PAH/VSG reprocessing of absorbed energy packets. Note that the PAH/VSG opacity is not negligible at long wavelengths, so even photons with just a few eV of energy can excite PAH emission, as described by Li & Draine (2002). The shape of the continuum emission in the 20–35 $\mu$m region is sensitive to the intensity of the illuminating radiation field, but the spectral shape and relative strengths of the PAH emission features are relatively insensitive to $U$ for $U < 10^4$ (see, e.g., Fig. 13 of Draine & Li 2007), where $U$ is the energy density of the radiation field relative to that of the interstellar radiation field of Mathis et al. (1983). Our reprocessing technique accounts for the fact that single photons may excite PAHs/VSGs in environments where the mean intensity is very low. Our technique also incorporates the effect of multiphoton excitation because the Draine & Li (2007) emissivity calculations include this effect, which becomes important in regions of high mean intensity.

## 3. GOMEZ'S HAMBURGER MODELS

Figures 3 and 4 show spectra and images of our model of Gomez's Hamburger that reproduce the observed spectrum and *HST* images. The broadband optical and near-infrared photometry, as well as the *IRAS* 60 $\mu$m flux, were taken from Ruiz et al. (1987). The Infrared Array Camera (IRAC) images and IRS spectrum were extracted from the *Spitzer Space Telescope* data archive (PI: C. Marwick-Kemper; program P01094). Aperture photometry was performed on the IRAC and Multiband Imaging Photometer for *Spitzer* (MIPS) 24 $\mu$m data, with the appropriate point-source aperture corrections applied. The source is slightly extended at IRAC wavelengths, but the *Spitzer* Science Center recommends that for extended sources smaller than 8″–9″ in size, the point-source corrections should be used. The *HST* WFPC2 images were extracted form the Multimission Archive at STScI (MAST) archive (PI: K. Noll, *HST* proposal 9315).

The model comprises a flared disk illuminated by a central star. The central star was spectroscopically identified as being A0 III by Ruiz et al. (1987), so we adopt $L_* = 160\ L_\odot$ and $T_* = 10^4$ K. The input spectrum is a $10^4$ K NextGen model atmosphere (Hauschildt et al. 1999). As mentioned earlier, the *HST* images resemble those of edge-on protoplanetary disks; therefore, we adopt a flared disk geometry for the circumstellar density structure parameterized by

$$\rho(r) = \rho_0 \exp\left[-\frac{1}{2}z^2/h(r)^2\right]\left(\frac{r}{R_*}\right)^{-\alpha} \quad (3)$$

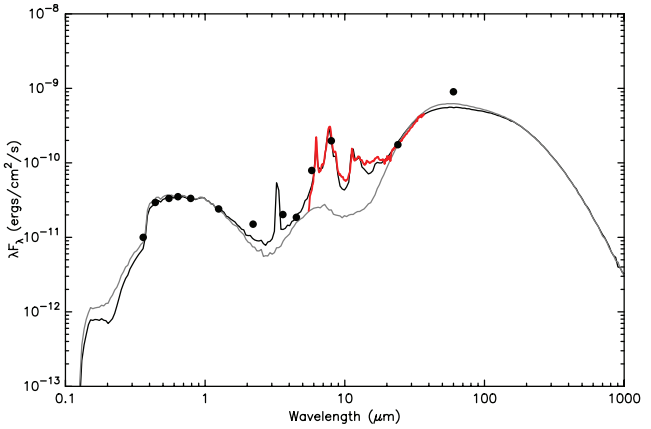


FIG. 3.—SED data (*dots and red curve*) and our best disk model (*upper solid line*) for Gomez's Hamburger. The lower solid line at mid-infrared wavelengths shows the same disk model without the PAH/VSG components.

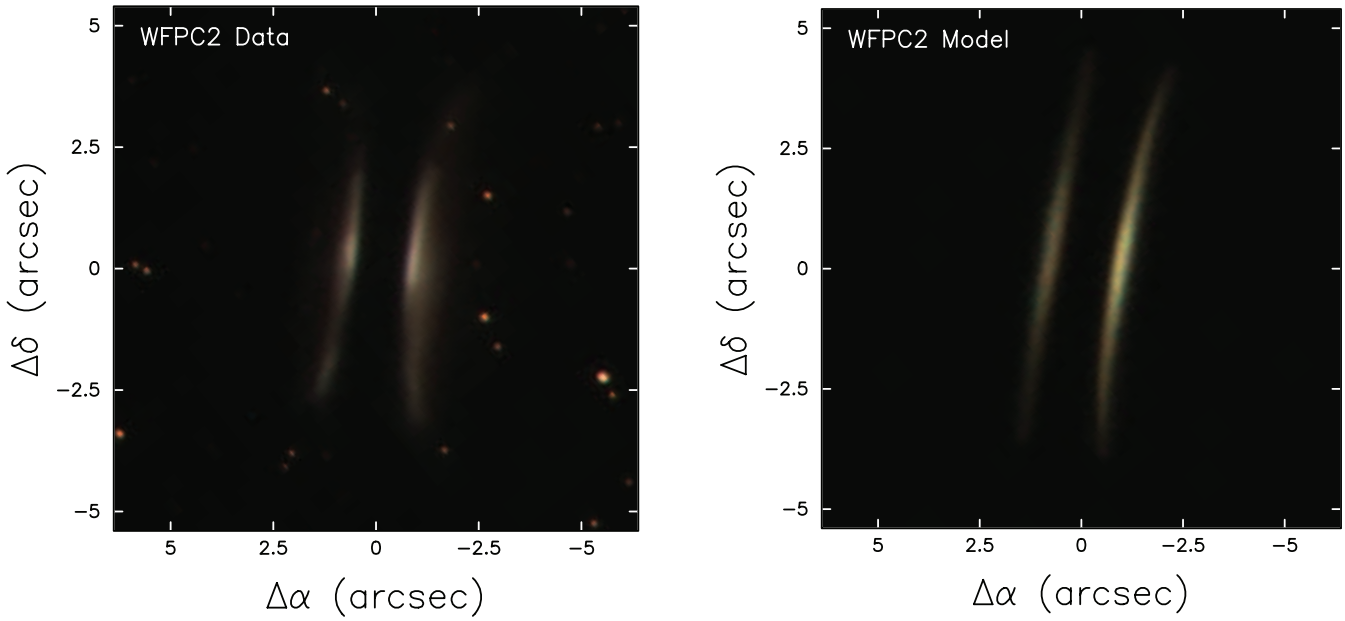


FIG. 4.—Three-color images at *B* (*blue*), *V* (*green*), and *R* (*red*) bands showing *HST* data (*left*) and model (*right*) images for Gomez's Hamburger.

for $r > R_{\rm min}$, where $r$ and $z$ are the cylindrical coordinates and $R_{\rm min}$ is the inner radius of the disk. The disk scale height $h(r) = h_0(r/R_*)^{\beta}$, where $h_0$ and $\rho_0$ are the scale height and density at the stellar radius, $R_*$. The surface density therefore has the form $\Sigma(r) \sim r^{\beta-\alpha}$. Models of disks heated by a central star typically yield surface densities $\Sigma \sim r^{-1}$ and flaring parameters in the range $1.1 \lesssim \beta \lesssim 1.3$ (see review by Dullemond et al. 2007b).

For the radiative equilibrium circumstellar dust, we adopt the opacity and scattering properties of the dust model described in Wood et al. (2002). This dust model extends to larger sizes than ISM grains and produces a shallower wavelength-dependent opacity. Larger grains are expected from theories of coagulation in disks, and this dust model gives a good representation of the SEDs of disks in Taurus (e.g., Rice et al. 2003). We use this dust model in the absence of millimeter observations of Gomez's Hamburger, which can help to determine the slope of the long-wavelength dust opacity and hence information on the dust size distribution.

In addition to a radiative equilibrium dust component we introduce the PAH/VSG opacity and emissivity as described above. The PAH/VSG component of the dust has the same radial density structure but is allowed to have a larger scale height from the radiative equilibrium grains. The scale heights ($h_0$) of the PAH/VSG and thermal dust components are parameters which are varied in a grid of models we ran to reproduce the observations (see below). This approximates dust settling in disks (see also Scholz et al. 2006) where the smaller grains (PAHs/VSGs in our model) have a larger scale height than the larger radiative equilibrium grains. Therefore the density structures of the PAHs/VSGs and radiative equilibrium grains are given by equation (3) with only the $\rho_0$ and $h_0$ terms differing to reflect the different mass fractions and scale heights of radiative equilibrium grains and PAHs/VSGs. The mass fraction of PAHs/VSGs is one of the free parameters in our modeling.

In our modeling procedure we ran a small grid of models to determine the distance to Gomez's Hamburger in addition to the disk mass, inner hole size, scale heights of the radiative equilibrium dust and PAH/VSG components, and the PAH/VSG fraction required to reproduce the features observed in the IRS spectrum. As the disk is observed to be close to edge-on, we restricted the inclination to be $i > 85^{\circ}$ because lower inclination disks produce a larger contrast between the upper and lower parts of the scattered light disk.

Assuming the illuminating source is an A0 III star and the circumstellar disk is viewed close to edge-on, allows us to determine the distance, interstellar extinction, and disk radius by fitting the optical flux levels and image size as shown in Figures 3 and 4. From this we determine $d = 280$ pc, $R_d = 1600$ AU, and $A_V = 1.8$. The disk inclination, flaring parameter ($\beta$), scale height, and mass of the radiative equilibrium dust component are determined from comparing models with the *HST* images. We varied these parameters in the range $85^{\circ} \leq i \leq 90^{\circ}$ and $1.1 \leq \beta \leq 1.3$.

The two SED models shown in Figure 3 are our best-fit models with and without PAHs/VSGs. We calculated goodness-of-fit $\chi^2$ values for the two models using broadband fluxes only and separately using only the IRS data. Assuming 15% errors on each data point, we find that for the broadband fluxes (13 data points) the model without PAH/VSG effects has $\chi^2 = 381.2$, while the model including PAHs/VSGs has $\chi^2 = 50.8$. Using only the IRS data (273 data points) gives $\chi^2 = 19,350$ (model without PAHs/VSGs) and $\chi^2 = 376$ (model including PAHs/VSGs). For the model including PAH/VSG effects and considering all the data, we find $\chi^2 = 1.49$ per data point, i.e., an average deviation of 1.22 $\sigma$.

Many degeneracies exist in modeling disk images and SEDs, notably in the disk flaring parameters $h_0$ and $\beta$. Within the context of the smooth, axisymmetric power-law disk structure model in the parameter space we explored, we found values that reproduce the infrared SED and images (Figs. 3 and 4) are $i = 87^{\circ} \pm 1^{\circ}$, $\beta = 1.2$, $M_{\rm dust} = 0.003 \pm 0.0005\ M_{\odot}$, and $h_0 = 0.0077 \pm 0.0005$. The value of $\beta$ together with our assumption that the surface density scales as $\Sigma \sim r^{-1}$ therefore gives $\alpha = 2.2$. Assuming a gas-to-dust ratio of 100 results in a total disk mass of 0.3 $M_{\odot}$. This disk mass is in excellent agreement with that determined from the CO observations of Bujarrabal et al. (2008), who derived a disk mass of 0.9 $M_{\odot}(d/500\ {\rm pc})^2$.

We allow the scale height of the PAHs/VSGs to differ from that of the larger radiative equilibrium grains and find that a

PAH/VSG mass fraction of $1.5\% \pm 0.25\%$ and scale height $h_0^{\rm PAH} = 0.009 \pm 0.001$ reproduce the *Spitzer* IRS spectrum as shown in Figure 3. The larger scale height for the PAH/VSG component is consistent with many other disk models that predict the coagulation and settling of large grains to the midplane. We also found that the IRS spectrum was best reproduced with an inner disk hole size of $R_{\rm min} = 500 \pm 25 R_*$, which is larger than the dust destruction radius of radiative equilibrium grains of $40 R_*$, assuming a typical dust sublimation temperature of 1600 K.

Figures 3 and 4 show that, compared to a model without PAHs/VSGs, our circumstellar disk model together with our new technique for incorporating PAH/VSG emission processes provides a very good match to the observed SED and high-resolution optical images of Gomez's Hamburger. In particular the relative strengths of the PAH features in the *Spitzer* IRS spectrum are well reproduced, whereas they are absent in the model without PAHs/VSGs. We do not fit the *IRAS* 60 $\mu$m data point, but this is not a great concern due to potential contamination problems with the *IRAS* data. In fact the *IRAS* 100 $\mu$m data are not usable for this source.

The PAH/VSG emissivities we use in our code were developed by Draine & Li (2007) specifically to model post-*Spitzer* data of the diffuse ISM in the Milky Way and other galaxies. Further applications of our code to model mid-infrared spectra of other disks will enable us to test whether the Draine & Li (2007) model can fit PAH features in a broad range of environments. Recent studies of PAH features in Herbig Ae stars (Boersma et al. 2008) suggest there are multiple components that differ from the ISM-like model we have adopted.

In Figure 3 we also show our disk model SED *without* PAHs/VSGs which are seen to dominate in the wavelength range $5\ \mu{\rm m} \lesssim \lambda \lesssim 20\ \mu$m and also with a strong feature around 3 $\mu$m. The excess emission from disks in this mid-infrared region is very sensitive to disk heating by viscous accretion. Therefore care must be taken when analyzing mid-infrared observations of disks, because radiation transfer models that do not include PAH/VSG emission could lead to overestimating the accretion rate in order to "fill in" the mid-infrared excess. High-resolution mid-infrared spectra that can identify PAH features will greatly assist in the analysis and interpretation of infrared spectra and accretion rates of protoplanetary disks.

In summary we find that if the central object is an A0 III star, then Gomez's Hamburger lies at a distance of 280 pc, much closer than the 2.9 kpc estimated by Ruiz et al. (1987). The nebulosity may be modeled with a highly inclined disk of mass 0.3 $M_\odot$ and radius 1600 AU. We reproduce the PAH features present in the *Spitzer* IRS spectrum using the PAH/VSG model and associated opacities and emissivities computed by Draine & Li (2007) for their model of the infrared spectrum of the diffuse ISM in our Galaxy.

Our modeling of the circumstellar structure suggests that Gomez's Hamburger is an edge-on protoplanetary disk around an A0 star. However, if the spectral type of the source is inaccurate, we cannot rule out the possibility that Gomez's Hamburger is much closer and the disk has a smaller radius (for a lower luminosity source). Conversely, a higher luminosity central source would yield a larger disk radius and distance. As the optical spectrum is entirely scattered light, the combination of high-resolution optical spectroscopy and radiation transfer modeling of the scattered starlight from the disk is required for more accurate spectral typing. The original suggestion from Ruiz et al. (1987) is that Gomez's Hamburger is a proto–planetary nebula. While our model does not explicitly address this scenario, our derived circumstellar disk structure is consistent with dynamical models of planetary nebulae requiring a preexisting circumstellar disk or torus which can act to focus and shape the stellar material ejected during the planetary nebula phase (e.g., Balick & Frank 2002).

## 4. SUMMARY

We have presented a straightforward method to include the absorption and reemission from PAH molecules and VSGs into Monte Carlo radiative equilibrium codes. Our technique utilizes precomputed intensity-dependent emissivities from which we sample the emission spectrum of Monte Carlo energy packets that have been absorbed by PAHs/VSGs. Our codes are readily adaptable to include a range of sizes for the PAHs/VSGs, but in this first paper we adopt a grain size cutoff of 200 Å, above which we assume the dust grains attain radiative equilibrium temperatures. For grain sizes smaller than 200 Å, absorbed energy packets are reprocessed using the precomputed emissivity files as described in § 2. Incorporating the PAH/VSG emission in this manner allows us to compute model spectra and images very quickly without repeating lengthy calculations of statistical equilibrium and transient heating and cooling of the PAH/VSG component—these calculations are in effect already incorporated in the precomputed PAH/VSG opacities and emissivities presented in Figures 1 and 2.

In a future paper we will extend our technique for sampling emissivities to be dependent not only on the intensity of the exciting radiation field, but also on the spectrum of the absorbed energy in each grid cell of our Monte Carlo simulation. Similar to the mean intensity calculation, determining the spectrum of the absorbed energy throughout our grid is straightforward to implement in Monte Carlo radiation transfer simulations. This more accurate treatment of the PAH/VSG reprocessing will be possible using planned calculations of PAH/VSG emissivity files for a range of exciting spectra comprising model stellar atmosphere spectra and blackbodies for a range of temperatures and reddening.

As a first application of our new code we modeled the object known as Gomez's Hamburger. We find that the broadband SED, high-resolution images, and *Spitzer* IRS spectrum can be reproduced with an edge-on circumstellar disk with a component of PAHs/VSGs comprising 1.5% of the dust mass. Our Monte Carlo radiation transfer using the adopted dust opacities ensures that very few high-energy photons penetrate into regions of large optical depth. Therefore there is little or no PAH/VSG emission from such regions, and the PAH/VSG emission is largely confined to a surface layer exposed to the direct stellar radiation. This is what is observed in the limb-brightened bubbles in the GLIMPSE survey (Churchwell et al. 2006). In future papers we will use our code to model the bubbles observed in the GLIMPSE survey to address the question of PAH/VSG survival around hot stars and in H II regions in addition to modeling the dust content within the H II regions and the effects this may have on determining the ionizing luminosity of the central sources. We will also investigate emission from PAHs/VSGs in protostars, thus extending the radiative equilibrium dust modeling presented by Whitney et al. (2003a).

T. R. is supported by a Scottish Universities Physics Alliance Studentship, B. A. W. is supported in part by the NASA Theory Program (NNG05GH35G), and B. T. D. was supported in part by NSF grant AST 04-06883.

REFERENCES

Balick, B., & Frank, A. 2002, ARA&A, 40, 439
Bjorkman, J. E., & Wood, K. 2001, ApJ, 554, 615
Boersma, C., Bouwman, J., Lahuis, F., van Kerckhoven, C., Tielens, A. G. G. M., Waters, L. B. F. M., & Henning, T. 2008, A&A, 484, 241
Bujarrabal, V., Young, K., & Fong, D. 2008, A&A, 483, 839
Burrows, C. J., et al. 1996, ApJ, 473, 437
Chakrabarti, S., & Whitney, B. 2007, ApJ, submitted (arXiv: 0711.4361v1)
Churchwell, E., et al. 2004, ApJS, 154, 322
———. 2006, ApJ, 649, 759
Draine, B. T., & Li, A. 2007, ApJ, 657, 810
Draine, B. T., et al. 2007, ApJ, 663, 866
Dullemond, C. P., Henning, T., Visser, R., Geers, V. C., van Dishoeck, E. F., & Pontoppidan, K. M. 2007a, A&A, 473, 457
Dullemond, C. P., Hollenbach, D., Kamp, I., & D'Alessio, P. 2007b, in Protostars and Planets V, ed. B. Reipurth, D. Jewitt, & K. Keil (Tucson: Univ. Arizona Press), 555
Geers, V. C., et al. 2006, A&A, 459, 545
Grosso, N., Alves, J., Wood, K., Neuhäuser, R., Montmerle, T., & Bjorkman, J. E. 2003, ApJ, 586, 296
Habart, E., Natta, A., & Krügel, E. 2004, A&A, 427, 179
Hauschildt, P. H., Allard, F., & Baron, E. 1999, ApJ, 512, 377
Indebetouw, R., Whitney, B. A., Johnson, K. E., & Wood, K. 2006, ApJ, 636, 362
Li, A., & Draine, B. T. 2002, ApJ, 572, 232
Lucy, L. B. 1999, A&A, 344, 282
Manske, V., & Henning, T. 1998, A&A, 337, 85
Mathis, J. S., Mezger, P. G., & Panagia, N. 1983, A&A, 128, 212
Misselt, K. A., Gordon, K. D., Clayton, G. C., & Wolff, M. J. 2001, ApJ, 551, 277
Peeters, E., Spoon, H. W. W., & Tielens, A. G. G. M. 2004, ApJ, 613, 986
Pontoppidan, K. M., Dullemond, C. P., Blake, G. A., Evans, N. J., II, Geers, V. C., Harvey, P. M., & Spiesman, W. 2007, ApJ, 656, 991
Rice, W. K. M., Wood, K., Armitage, P. J., Whitney, B. A., & Bjorkman, J. E. 2003, MNRAS, 342, 79
Ruiz, M. T., et al. 1987, ApJ, 316, L21
Scholz, A., Jayawardhana, R., & Wood, K. 2006, ApJ, 645, 1498
Whitney, B. A., & Hartmann, L. 1992, ApJ, 395, 529
Whitney, B. A., Wood, K., Bjorkman, J. E., & Cohen, M. 2003a, ApJ, 598, 1079
Whitney, B. A., Wood, K., Bjorkman, J. E., & Wolff, M. J. 2003b, ApJ, 591, 1049
Wood, K., Lada, C. J., Bjorkman, J. E., Kenyon, S. J., Whitney, B., & Wolff, M. J. 2002, ApJ, 567, 1183